Derivation of Aqua MODIS Polarization Correction

June 1, 2004

Gerhard Meister, NASA Goddard Space Flight Center , Code 970.2, OCDP
(meister@simbios.gsfc.nasa.gov, 301-286-0758)

Contents

1 Abstract

This report describes the methods used to derive the MODIS Aqua polarization correction from the prelaunch measurements for the OCDP reprocessing.

2 Introduction

This document follows conventions used in [1]. The correct conversion of the angles of the polarizer of the prelaunch measurements to the coordinate system used in the level 2 code polarization correction is now being used, i.e. the information regarding the rotation of the polarizer from [3] is no longer used. It is anticipated that the polarization correction presented here will be improved in the future by further analysis.

3 Prelaunch Measurements

3.1 Footprint of the polarized signal

The image of the polarizer covers the 10 detectors of the MODIS ocean bands and is about 10 frames wide at the center detectors, about 5 frames for the outer detectors. The image moves by up to 1 or 2 pixels up and down for different rotation angles of the polarization filter. MCST has accounted for this by only using those 3 consecutive frames with the maximum values. This algorithm has been applied in this report as well.

3.2 Discussion of measurement artifacts

A look at the detector specific signals for band 8 in Fig. 1 shows a strong variation of the signal for the different detectors. It is interesting to note that neither the phase nor the magnitude seem to vary strongly for the different detectors, the variation affects mainly the measurements around 0°, which are lower than the measurements around ±180° for detector 10, but similar to the measurements around ±180° for detector 1. This suggests that the detector-to-detector variations are calibration artifacts, and a band specific polarization correction might give better results than a detector specific correction.

The expected result of the polarization measurements is a signal with two cycles over the range of rotation angles β of the polarizer from $-180°$ to $+180°$. The expected function $v_e(\beta)$ can be described by

$$v_e(\beta) = a_0 + a_1 \cdot \cos(2\beta - \delta) \tag{1}$$

There are several issues that are disturbing (see Fig. 6 below):

- **There is no dominant two cycle pattern in many bands, only bands 8, 9 and 16 show a clear two cycle pattern for all viewing angles.** This suggests that measurement artifacts dominate the signal in bands 10-15.
- **For bands 8,9, and 16, a rotation of the polarizer by** 180° **changes the measured value, although the effect should be zero.** The average difference is between 2.0 and 2.5% for a viewing angle of 45°, which is a significant portion of the total effect (difference

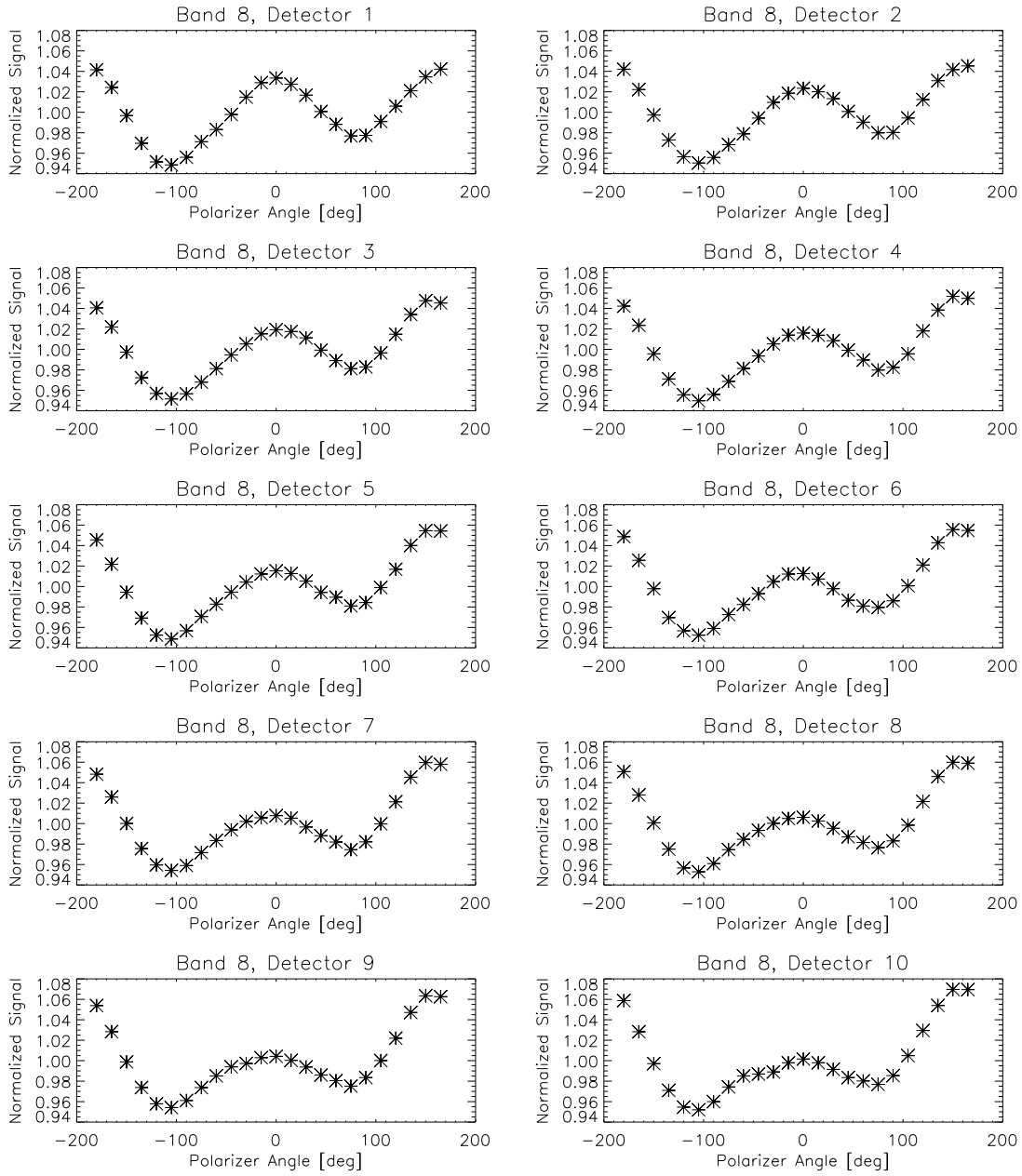

Figure 1: Prelaunch polarization measurements of Aqua MODIS band 8 for mirror side 1. The plots show the Aqua MODIS prelaunch polarization measurements for each detector (in product order) for a viewing angle of $-45°$, corresponding to an incidence angle on the scan mirror (AOI) of $15.5°$.

between maximum and minimum is 13.5% for band 8, 8% for band 9 and 7.5% for band 16). This means even for bands 8, 9 and 16 strong calibration artifacts are present.

- [2] suggest to retrieve the 'true' polarization pattern with Fourier analysis for those bands showing a four-cycle component (bands 13-15), keeping only those components corresponding to the two-cycle effect. The four-cycle effect seems to be larger than the two-cycle effect in the Aqua data. **It is not clear that with other calibration artifacts and measurement noise interfering, the two-cycle effect can be correctly extracted from the Aqua data for bands 13-15.**

4 Setup in the SBRS Laboratory

The setup presented in Figs. 2 and 3 is based on information from Gene Walushka and Jack Xiong. It is the basis for the current polarization LUT. The initial operational LUT (before 2003) was based on a setup with MODIS turned by 90°. The initial operational LUT results in corrections that are opposite to the current LUT, see section 8 below.

The prelaunch polarization measurements were provided by MCST for several rotation angles β of the Polarization Spectral Assembly (PSA). The position of MODIS relative to the PSA is needed to convert the angles on the PSA into angles in the MODIS coordinate system as defined by SBRS. In Figures 2 and 3, the rotation angle β of the PSA is shown relative to the MODIS coordinate system. The MODIS x-axis is parallel to the rotation axis of the scan mirror, with the positive x-axis pointing into the flight direction. The positive MODIS z-axis is pointing to the earth view, or in this case the PSA. The MODIS coordinate system is right-handed, i.e. $\hat{x} \times \hat{y} = \hat{z}$. In both figures, the setup is shown for a MODIS viewing angle of 0° (measurements were done at $-45°, -22.5°, 0°, 22.5°, 45°$).

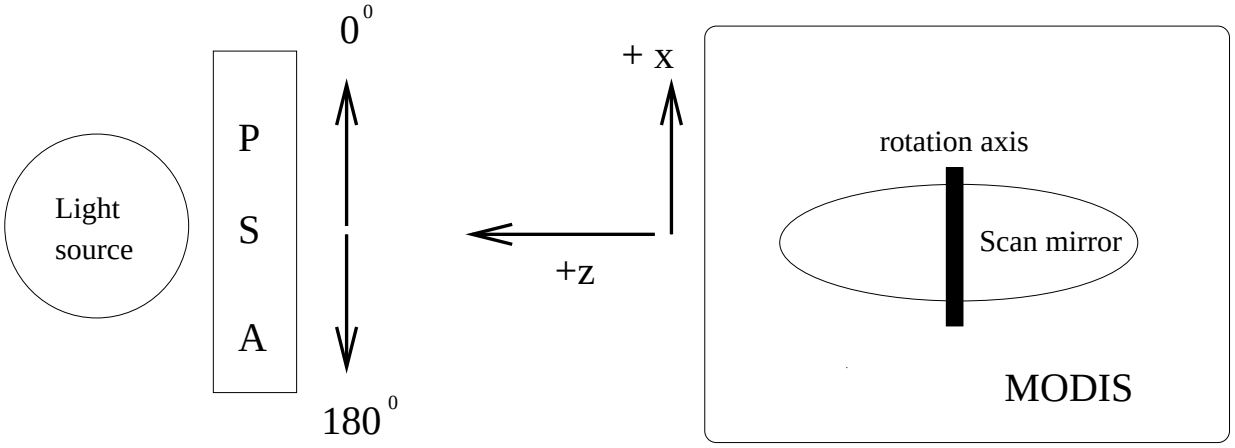

Figure 2: Rotation angles $\beta = 0°$ and $\beta = 180°$ of the PSA (left) relative to the MODIS coordinate system as defined by SBRS, view of the setup in the SBRS laboratory from the **side**. The x-axis points into the MODIS flight direction.

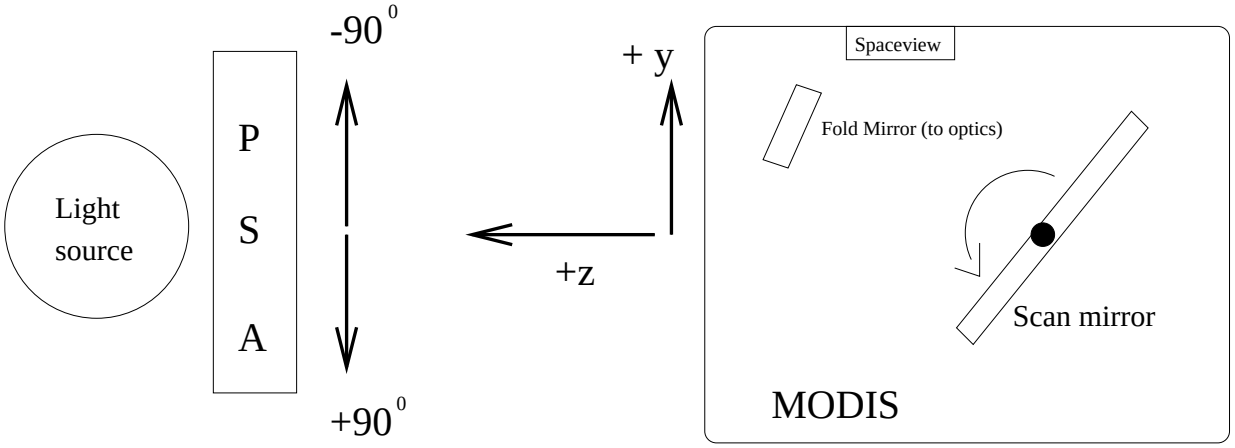

Figure 3: Rotation angles $\beta = +90°$ and $\beta = -90°$ of the PSA relative to the MODIS coordinate system, view of the setup in the SBRS laboratory from the **top**. The dark circle in the center of the scan mirror is the rotation axis of the scan mirror. The space view port is seen by the scan mirror when looking approximately to the top (+y axis). The scan mirror rotates counterclockwise in this plot around the x-axis (positive direction as defined by the right hand rule). For the measurements at a viewing angle of $-45°$, MODIS was rotated counterclockwise in this plot by $45°$ around the rotation axis of the scan mirror. The space view port is located approximately in the direction of the y-axis.

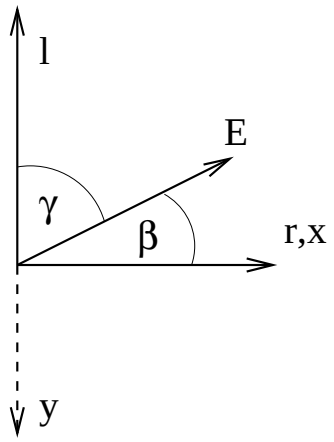

Figure 4: The electric field vector $\vec{E}$ in the level 2 code coordinate system (r, l) and the MODIS coordinate system (x, y) as defined by SBRS. The propagation direction of light is from the plot towards the viewer, corresponding to the z'-axis.

5 Transformation to reference frame of level 2 code

Ultimately, the rotation angles of the polarizer need to be converted into the reference frame that was used in the level 2 code, where the polarization correction is applied to the earth-view data. From information provided by Howard Gordon, we derived that the following coordinate system (r,l,z') was used in the level 2 code:

- r-axis in level 2 code parallel to x-axis in Fig. 2.
- z'-axis in level 2 code anti-parallel to z-axis in Fig. 2.
- l-axis in level 2 code anti-parallel to y-axis in Fig. 3.

The coordinate system in the level 2 code is right-handed, i.e. $\hat{r} \times \hat{l} = \hat{z'}$. Fig. 4 compares the level 2 code coordinate system to the MODIS coordinate system as defined by SBRS.

The rotation angle β on the PSA was converted to the angle γ in the coordinate frame of the level 2 code (where γ is the angle relative to the l-axis of the reference frame in the level 2 code, i.e. with $\gamma = 0°$ pointing into the direction of the l-axis , $\gamma = 90°$ pointing into the direction of the r-axis, see Fig. 4) using the following formula:

$$\gamma = -\beta + 90° \tag{2}$$

(This transformation has been used in the time series AT06 by the OCDP group.) The angle γ will be used in section 6, where the polarization coefficients will be calculated.

6 Calculation of the correction parameters

A Stokes vector of intensity I_t as defined in [1], eq. 1, of linearly polarized light can be calculated as (see [4], page 27)

$$\begin{aligned} I &= I_t \\ Q &= I_t \cdot \cos(2 \cdot \gamma) \\ U &= I_t \cdot \sin(2 \cdot \gamma) \\ V &= 0 \end{aligned} \tag{3}$$

with γ defined in Fig. 4.

The Stokes vector in the level 2 code is defined with respect to the (earth-) surface normal. The polarization correction parameters are determined in a coordinate system fixed with respect to MODIS. The transformation between these two coordinate system is accomplished by a rotation matrix containing the angle α, see [1]. For the prelaunch measurements, $\alpha = 0°$.

The polarization correction is contained in the variables m_{12} and m_{13} of eq.7 in [1]. In the level 2 code, these two variables correspond to the parameters am12 and am13, stored in an HDF LUT. Eq.7 in [1] with $\alpha = 0°$ yields

$$I_m = I + am12 * Q + am13 * U \tag{4}$$

where I_m is the uncorrected radiance measured by MODIS, I, Q, U are given by eq.3. The intensity I_t of the Stokes vector is approximately equal to the average of the measured radiances I_a:

$$I_a \equiv \sum_{i=1}^{n} I_m(\gamma) \approx I_t \tag{5}$$

where n is the number of measurements of I_m, 24 in the case of Aqua. The parameters am12 and am13 were fitted to the normalized prelaunch measurements $y(\gamma) = I_m/I_a$ with the following formula (derived from dividing eq. 4 by I_a and using eq. 3):

$$y(\gamma) = 1.0 + am12 \cdot \cos(2 \cdot \gamma) + am13 \cdot \sin(2 \cdot \gamma) \tag{6}$$

The IDL 'regress' routine was used to determine the parameters. For most bands, the results are identical if a Fourier transformation is used. Small differences appear for those bands that have a four-cycle component (see section 3.2 above). The use of a Fourier transformation was suggested for these bands by [2]. We plan to evaluate whether the correction from the Fourier transformation results in a more reasonable correction. Preliminary results show that the effect is negligible. The parameters am12 and am13 were calculated for each band, detector, viewing angle, and mirror side, resulting in $11 \times 10 \times 5 \times 2 = 1100$ sets of parameters.

The polarization correction LUT also contains two derived quantities, the polarization magnitude P_m and the polarization phase angle P_p, defined here as

$$P_m = \sqrt{am12^2 + am13^2} \tag{7}$$

and

$$P_p = -\text{atan}(\frac{am13}{am12}) \tag{8}$$

Although they are not used in the level 2 code, they were reproduced for the LUT to facilitate the quality control algorithm described in the following section. The polarization correction reaches a maximum or minimum at $\gamma_0 = -P_p/2$.

7 Band specific optimization

As described in section 3.2, the detector specific variations are likely measurement noise. The choice which detector to use as representative was made using the following criteria:

- The residuals between the prelaunch measurements and the fitted two-cycle effect should be small.
- The polarization magnitude P_m should increase with increasing AOI on the scan mirror.
- The variation of the phase angle P_p with AOI on the scan mirror should be small.

Table 1 shows which detectors were selected for each band. In some cases, no detector for a given angle satisfied the above criteria well, in this case the measurements from a different angle were chosen. These choices are documented in table 1 as well. The resulting polarization magnitudes and polarization phase angles are shown in tables 2 and 3. Bands 13H and 14H were set to 13L and 14L, respectively since the high gain bands were not yet investigated thoroughly (they may actually provide better data than the low gain bands).

Fig. 5 shows the measured prelaunch data for all 10 detectors of band 10 for a viewing angle of $+45^\circ$ and compares the fits to the individual detector data to the fit of detector 1, which was chosen to be representative for all detectors, see table 1. It can be seen that there are quite significant differences (up to about 1%) between curves fitted to the individual detectors and the curve fitted to detector 1, see e.g. detector 7. There is no certainty that the curve of detector 1 actually is a better approximation to the true polarization sensitivity of detector 7 than the curve fitted to the detector 7 data. The assumption that the detector-to-detector variability of the true polarization sensitivity is smaller than the measured detector-to-detector variability needs to be validated with ocean-color data, with one obvious criteria being the amount of striping introduced or removed by the assumption. In the case of detector 7 in Fig. 5, it is obvious that the non-two-cycle variability is much larger than the fitted two-cycle effect. This makes it unlikely that the two-cycle effect can be correctly retrieved from the data. Thus it seems more reasonable to use the two-cycle effect from

Band	$-45°$	$-22.5°$	$0°$	$+22.5°$	$+45°$
8	1	1	1	1	1
9	1	1	1	1	1
10	1 ($+45°$)	1 ($+45°$)	1 ($+45°$)	1 ($+45°$)	1
11	10 ($-22.5°$)	10	10	10	10
12	5	5	5	5	5 ($+22.5°$)
13L	10 ($-22.5°$)	10	10	10	10
14L	1	1	1	1	1
15	7	7	7	7	7
16	3	3	3	3	3

Table 1: The detectors in product order whose prelaunch measurements were chosen to derive the polarization correction coefficients for different viewing angles. If a bracket follows the detector number, a detector of the measurements from the angle in the bracket was chosen instead of a detector from the current angle. E.g., in band 10, the coefficients for all angles were set to those derived from detector 1 at a viewing angle of $+45°$.

Band	$-45°$	$-22.5°$	$0°$	$+22.5°$	$+45°$
8	0.0370104	0.0419231	0.0444085	0.0493411	0.0543175
9	0.0178488	0.0212673	0.0221404	0.0219310	0.0304233
10	0.0111656	0.0111656	0.0111656	0.0111656	0.0111656
11	0.00810166	0.00810166	0.00737253	0.00936571	0.0126522
12	0.0199038	0.0124699	0.0121134	0.00961104	0.00961104
13L	0.00759082	0.00759082	0.00708113	0.00767564	0.00770792
14L	0.00643985	0.00879929	0.00808135	0.0103178	0.0118745
15	0.00703764	0.00502653	0.00508441	0.00408902	0.00441548
16	0.0145901	0.0137505	0.0156766	0.0187032	0.0248304

Table 2: The polarization magnitude P_m for different viewing angles, calculated with $P_m = \sqrt{am12^2 + am13^2}$, averaged over both mirror sides.

Band	$-45°$	$-22.5°$	$0°$	$+22.5°$	$+45°$
8	9.99717	8.34773	8.98063	8.33345	7.32100
9	16.3167	12.1410	14.3183	14.6492	11.5337
10	8.17594	8.17594	8.17594	8.17594	8.17594
11	25.1143	25.1143	22.9555	18.8338	12.2644
12	5.16694	7.74336	8.68067	9.15911	9.15911
13L	37.5140	37.5140	34.2956	25.1115	16.1342
14L	10.4793	8.05184	10.5573	10.0928	9.91463
15	-1.40232	0.461974	2.84969	0.723078	4.55391
16	6.43282	7.34681	6.80166	5.29983	5.54587

Table 3: The polarization phase angles P_p in degrees for different viewing angles, calculated with $P_p = -\text{atan}(\frac{am13}{am12})$, averaged over both mirror sides.

detector 1 for detector 7, because for detector 1 we can see reasonable agreement between fit and measured data.

Fig. 6 shows the measurements that were used to derive the polarization correction for nadir viewing for all bands. For some bands (e.g. band 11) even the best detectors do not show a clear two-cycle effect. The four-cycle effect in bands 13,14, and 15 seems to be stronger than the two-cycle effect, casting serious doubts on the retrieved polarization sensitivity. Table 4 gives a rough estimate of the absolute error for all bands for nadir viewing. In some bands, the error is unacceptably high.

8 Comparison to previous correction

Fig. 7 compares the polarization correction calculated with the LUT 'modis-pol-corr-aqua-1a.hdf' used in the initial operational processing (R1), and the polarization correction calculated with the LUT 'modis-pol-corr-aqua-2c.hdf' used in the AT06 time series and the current operational processing. 'modis-pol-corr-aqua-1a.hdf' was provided by Jim Brown from the Miami group, 'modis-pol-corr-aqua-2c.hdf' was derived as explained in this report. It can be seen that typically the amplitude of the correction of the new correction is larger, and the phase is opposite in most cases.

Both LUTs have been used to create comparisons between the time series of the Aqua and SeaWiFS normalized water leaving radiances. The polarization correction affects the high latitude regions most, so in this report the results for only three regions in the pacific are shown: latitudes from $40°$ to $50°$ south (Fig. 8) and north (Fig. 9), and an equatorial region (Fig. 10), with longitudes from $150°$ to $170°$ for all three regions. It can be seen that the huge oscillations in the ratios between the Aqua and the SeaWiFS time trends for the high latitude regions have been significantly reduced, with the largest improvement in the northern high latitudes. There is still a much smaller oscillation in the time trends that is currently being investigated. The differences seen in the equatorial region

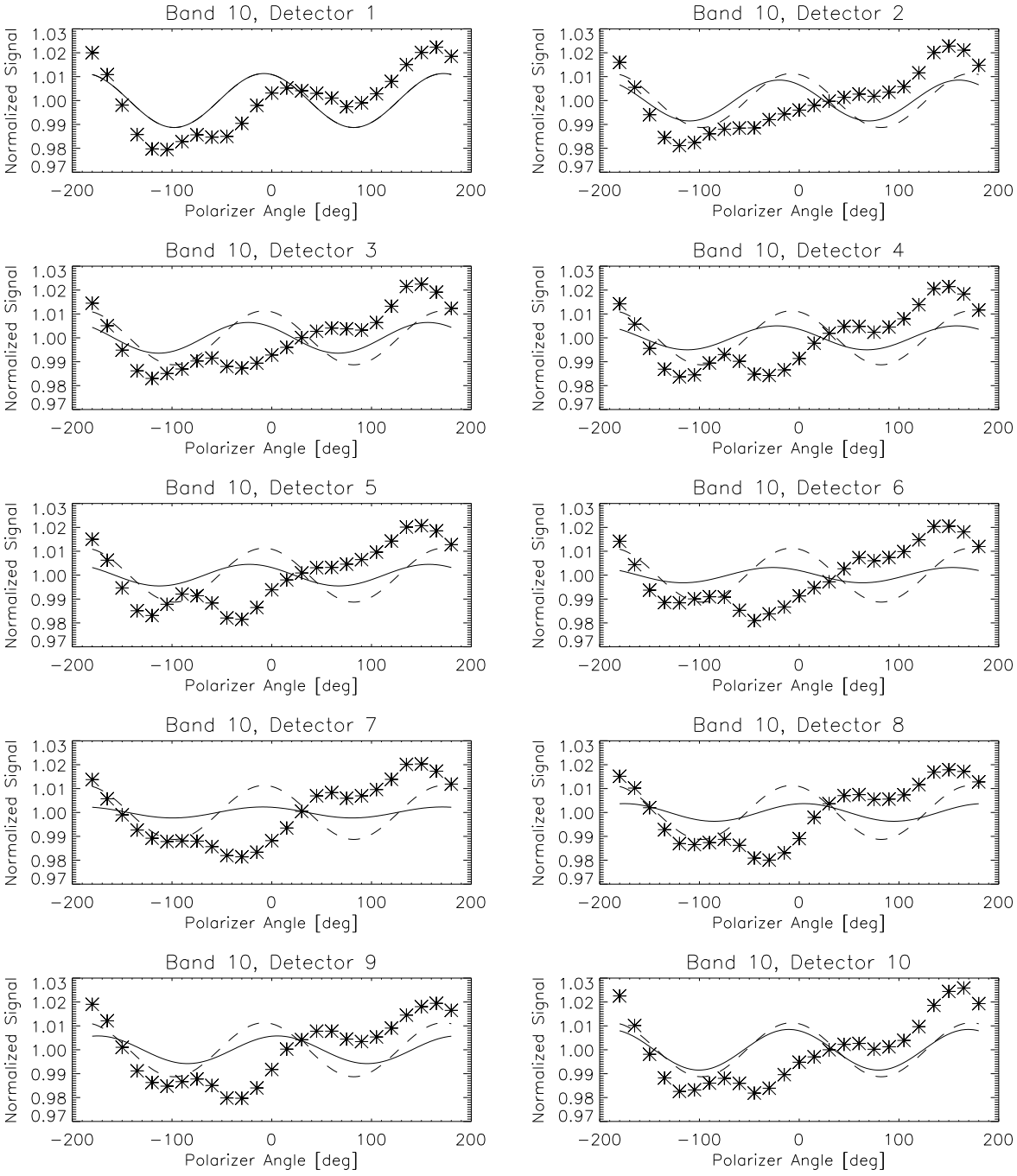

Figure 5: Prelaunch data for a viewing angle of +45° (mirror side 1) of band 10 for all 10 detectors. Stars show the measurements, the solid lines show the fit to the data of the respective plot. The dashed lines show the fit to detector 1.

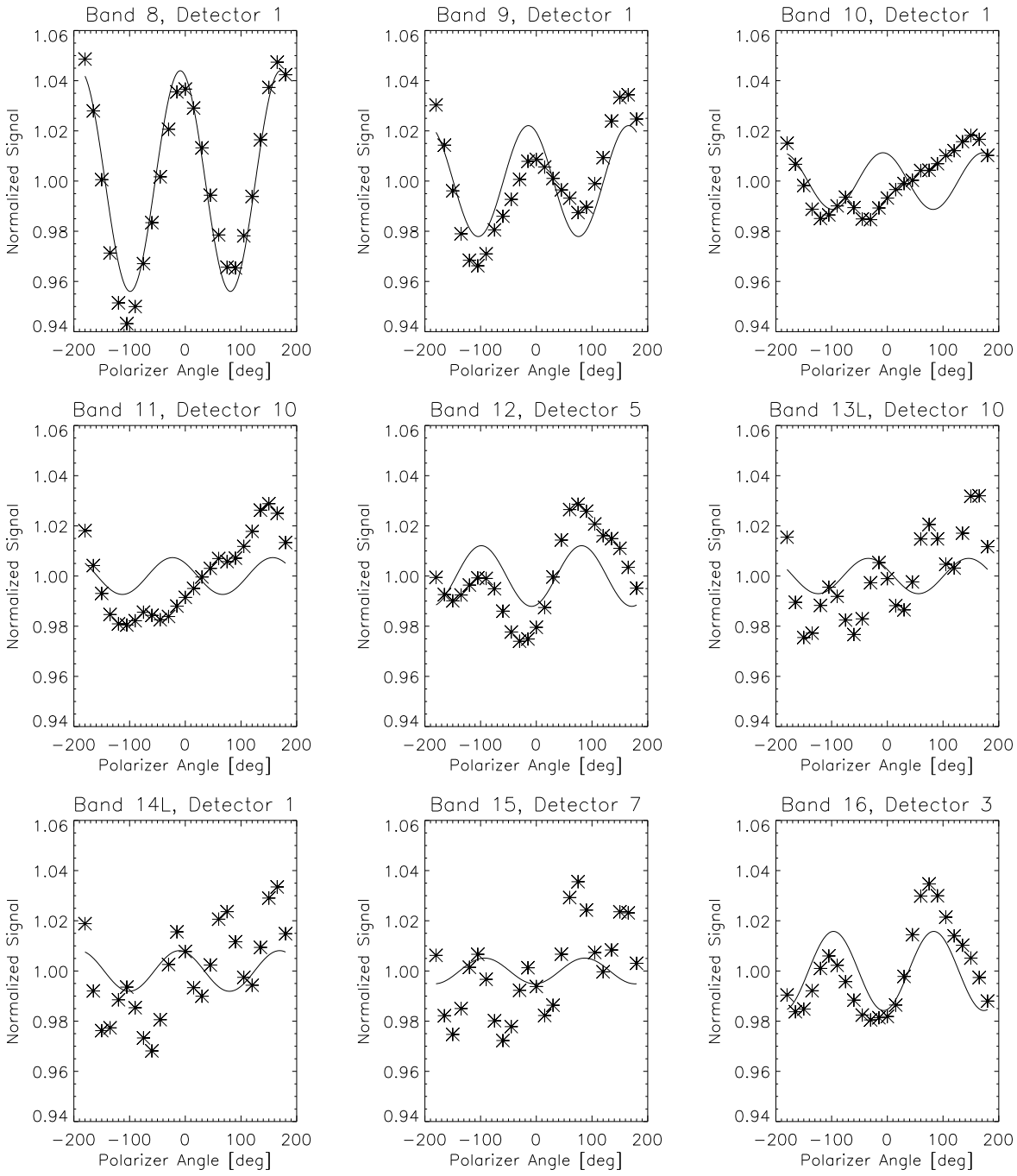

Figure 6: Prelaunch data used to derive the polarization correction for nadir viewing (mirror side 1) for all bands. Stars show the measurements, the solid lines show the fit to the measurements.

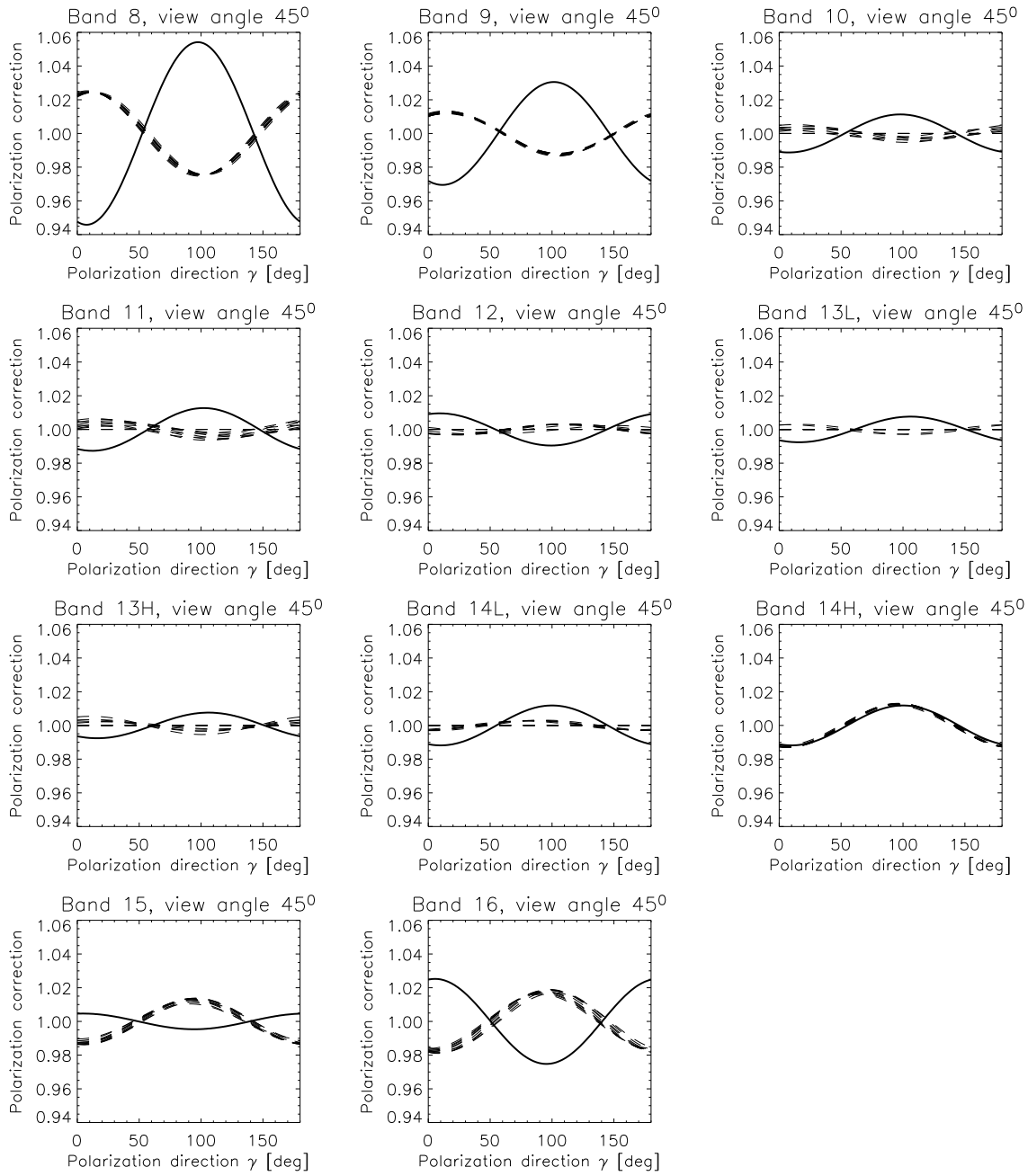

Figure 7: Polarization correction as a function of direction of polarization γ for viewing angle of $+45°$ (AOI on scan mirror of $60.5°$). The thick solid line is the current polarization correction (detector independent), the thin dashed lines show the polarization correction of the initial operational polarization correction (one line for each detector).

	Error
Band 8	0.002
Band 9	0.005
Band 10	0.010
Band 11	0.008
Band 12	0.010
Band 13L	0.010
Band 14L	0.010
Band 15	0.010
Band 16	0.005

Table 4: A rough estimate of the absolute error of the polarization correction for nadir viewing. A value of 0.010 means that if the polarization correction results in a value of 1.02, the true value is expected to be within 1.01 and 1.03.

are mostly due to an improved m1 LUT that has been used in the current processing. There is still a relatively strong disagreement in the northern latitude around January 2003 for band 8. It is possible that the atmospheric correction algorithm is insufficient to correct band 8 due to the high polarization sensitivity of band 8, even if the polarization sensitivity of band 8 has been well characterized.

References

[1] Gordon, H.R., Tao Du, Tianmin Zhang, *Applied Optics*, 1997, Vol. 36, No. 27, 6938-6948.

[2] Young, J., Knight, E., Merrow, C., SPIE Conference on Earth Observing Systems III, San Diego ,California, July 1998, SPIE Vol. 3439, 247-256

[3] Walushka, E., MODIS Polarization Measurements and Simulation and the 4θ Effect, In SPIE Vol. 3121, 1997

[4] Chandrasekhar, S., Radiative Transfer, Dover Publications Inc., New York, 1960

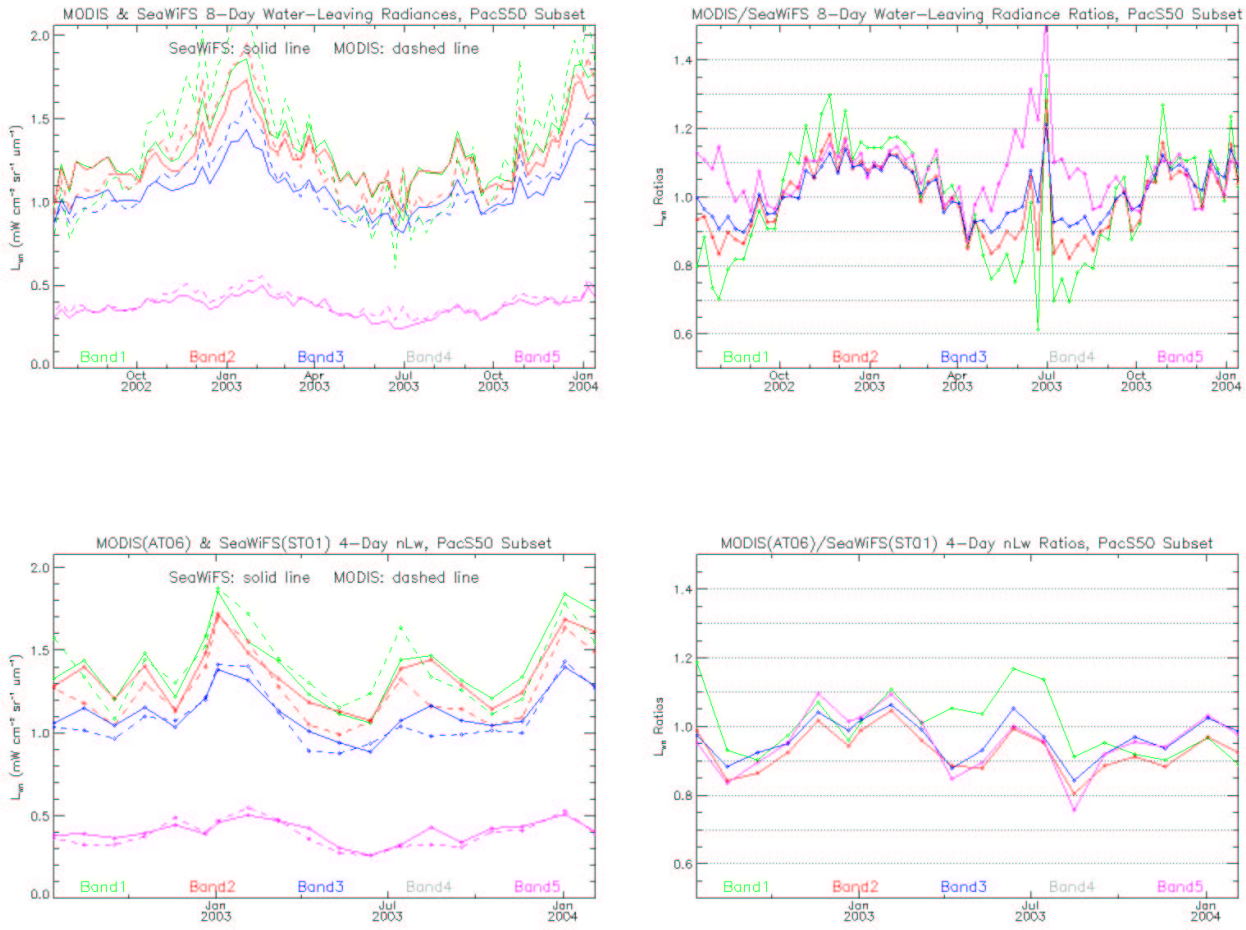

Figure 8: Time series of the water leaving radiances for the initial processing (top row) and the AT06 test (bottom row, same polarization LUT as in current processing) for high latitudes in the southern pacific. The left column shows the actual time series, the right column shows the ratio Aqua over SeaWiFS. All ocean color time series plots were provided by Bryan Franz.

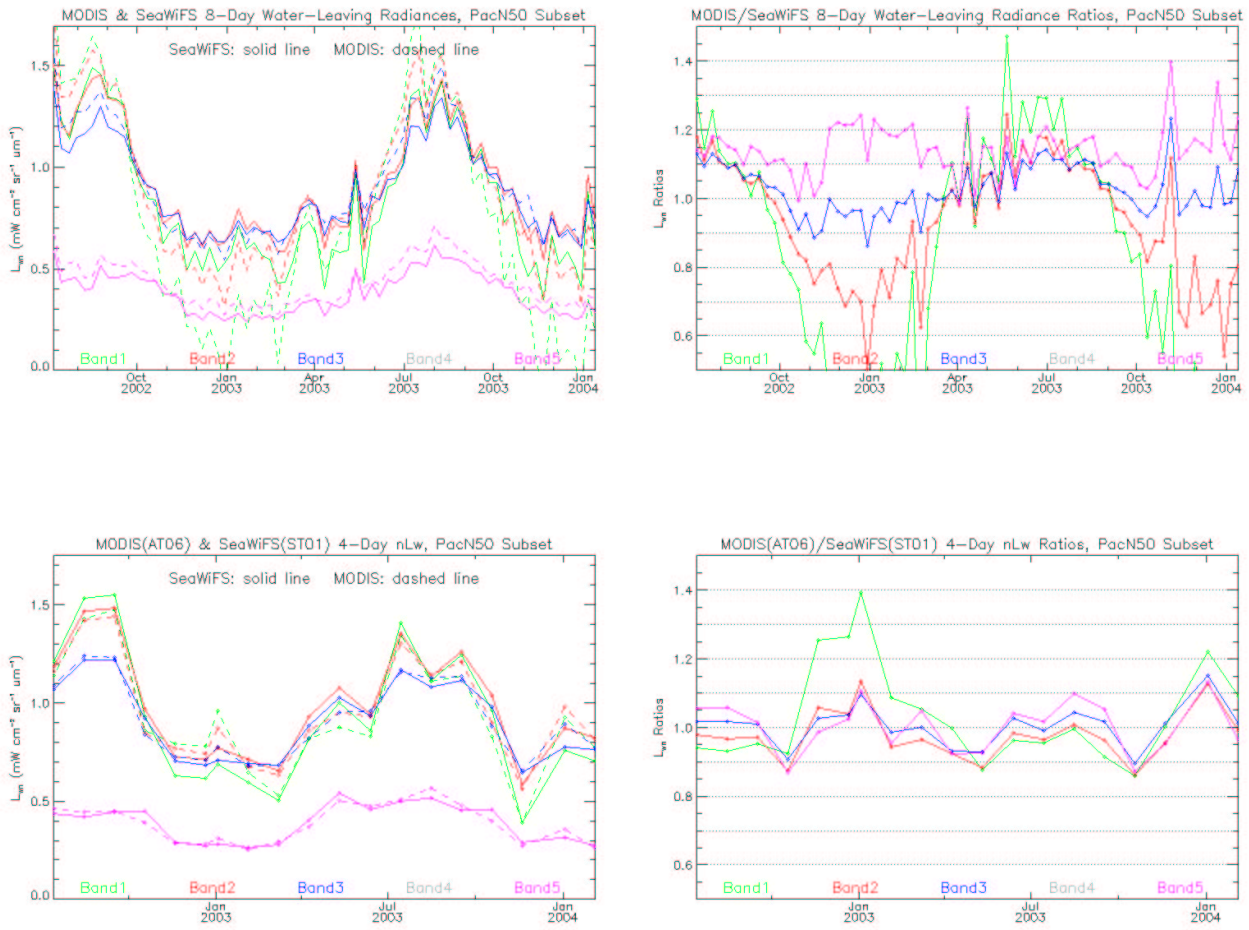

Figure 9: Same as Fig. 8 for northern pacific.

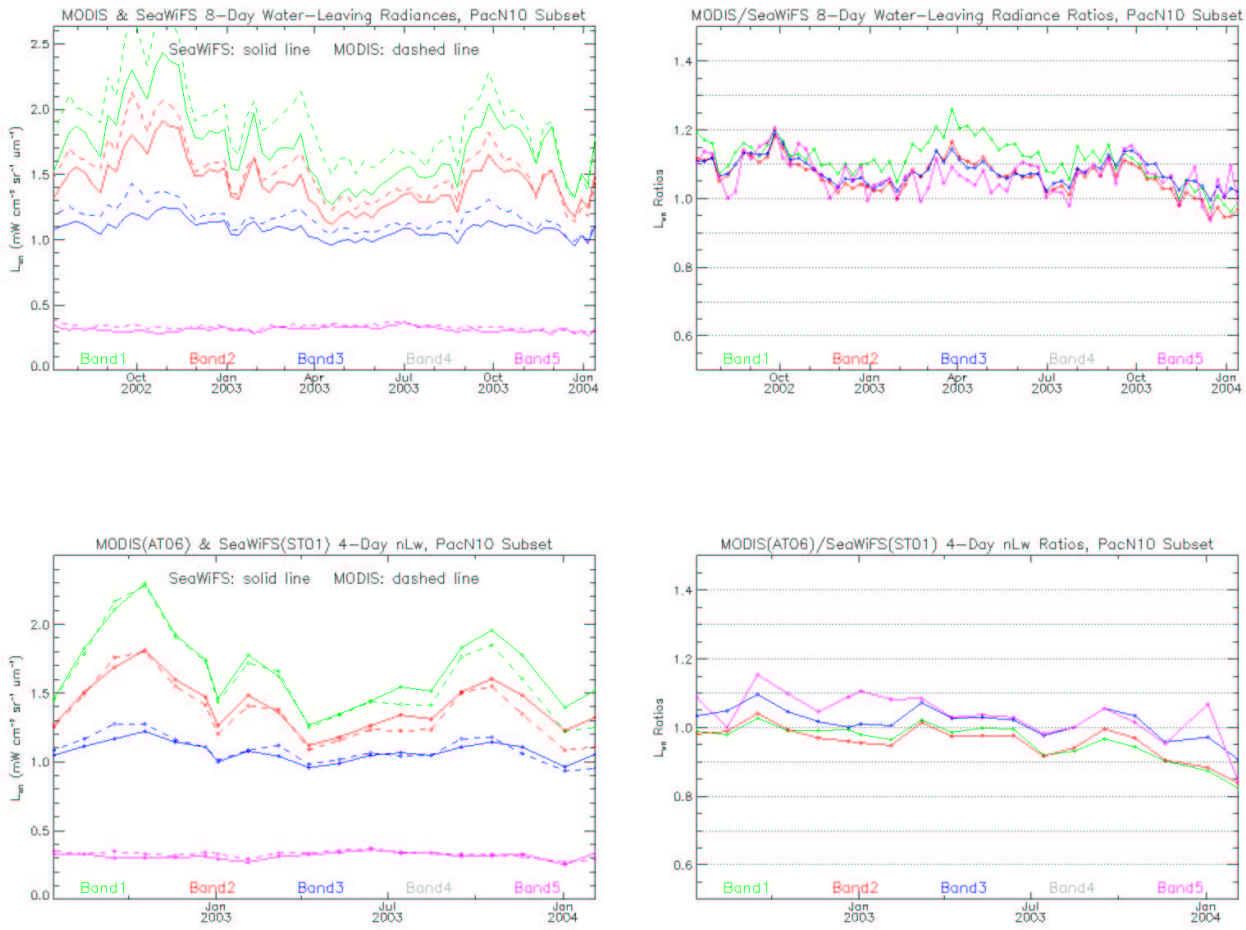

Figure 10: Same as Fig. 8 for equatorial pacific.